Journal of Power Sources 206 (2012) 253–258

Contents lists available at SciVerse ScienceDirect

Journal of Power Sources

journal homepage: www.elsevier.com/locate/jpowsour

Germanium nanowires-based carbon composite as anodes for lithium-ion batteries

Li Ping Tan [a], Ziyang Lu [a], Hui Teng Tan [a], Jixin Zhu [a], Xianhong Rui [a,b], Qingyu Yan [a,c], Huey Hoon Hng [a,c,*]

[a] School of Materials Science and Engineering, Nanyang Technological University, Singapore 639798, Singapore
[b] School of Civil and Environmental Engineering, Nanyang Technological, University, Singapore 639798, Singapore
[c] Energy Research Institute @ NTU, Nanyang Technological University, Singapore 638075, Singapore

ARTICLE INFO

Article history:
Received 4 November 2011
Received in revised form 5 December 2011
Accepted 7 December 2011
Available online 25 January 2012

Keywords:
Germanium nanowires
Porous carbon
Composite
Solution–liquid–solid
Lithium ion batteries

ABSTRACT

Lithium-ion batteries have been actively researched in recent years due to it being one of the most promising energy storage systems. Herein, we report a novel approach where germanium nanowires (Ge NW) are grown in gold-seeded porous carbon via the solution–liquid–solid mechanism, and the corresponding improvement observed in terms of the specific capacity of this porous carbon–germanium nanowires (PC–Ge NW) composite anode. At a current density of 160 mAg^{-1} and voltage window of 0.001–1.5 V, a specific capacity of 789 $mAhg^{-1}$ during the 50th cycle for PC–Ge NW is achieved as compared to 624 $mAhg^{-1}$ during the 50th cycle for pure Ge NW. Even though the content of the Ge is only 53.5 weight percent in the PC–Ge NW composite, it yields a better stability and higher specific capacity, indicating a synergistic effect between porous carbon and Ge nanowires. There is also potential cost savings since the use of a lower amount of Ge can bring about good cycling properties.

1. Introduction

Rechargeable lithium-ion batteries (LIBs) are widely used in applications like cell phones, laptops, and digital cameras, and much focus has been placed on LIBs research in recent years due to fact that it is one of the most promising energy storage systems with high energy density and long cycling lifetime. Coupled with the development of electric vehicles and hybrid electric vehicles, there is increased demand for LIBs with better performance for higher energy and power densities [1].

Current lithium-ion technology is based on a layered $LiCoO_2$ cathode and graphite anode [2]. Graphite is used as it has good capacity retention and low operating voltage; however, due to its low theoretical capacity of 372 $mAhg^{-1}$ (for LiC_6) [3], there are many studies on improving the anode material of LIBs. The desired properties of anode materials in LIBs are the ability to store a large amount of lithium while maintaining good cyclability and high rate capability [4], and research has been predominantly focused on lithium alloys [5].

Germanium (Ge) is amongst the most promising alternative anode materials due to their high theoretical capacity of 1600 $mAhg^{-1}$ for the alloy $Li_{22}Ge_5$ [6], and the reaction mechanism is as shown: $yGe + xLi^+ + xe^- \leftrightarrow Li_xGe_y$. Ge is analogous to Si, but it is seldom investigated due to concerns on its cost. This is because Ge is not widely available – it ranks near 50th in relative abundance of the elements in the Earth's crust, while Si is the 2nd most abundant material on earth. Thus, the supply for Ge is greatly limited by the availability of exploitable sources, and in turn affecting its cost. Ge is not known to be toxic, but can pose some hazards to human health. Nevertheless, compared to Si, Ge has about 400 times higher lithium diffusivity at room temperature, and less significant specific volume change during lithiation/delithiation [7]. The synthesis methods of Ge materials for LIB are commonly physical processes, e.g. ball milling [7], pyrolysis [8] and co-evaporation [9], and vapour–liquid–solid (VLS) mechanism [10], although some solution phase synthesis are reported as well [11,12].

Despite the high capacity, pure Ge anode also exhibits rapid capacity loss accompanied by a huge irreversible capacity due to the drastic volume change of the active material. This results in the pulverization of large particles and loss of the electrical contact between these particles and the current collector, leading to poor cyclability [7]. To mitigate this problem, several strategies have been proposed: (1) decreasing the active material's particle size [13,14], (2) dispersing the active material into an inactive/active buffer matrix [15,16], (3) synthesizing porous active materials [17,18], (4) using amorphous active materials [13,19], and (5) forming composites with conductive carbon [20,21].

Recently there have been quite a few reports on carbon based composites [22–26] and its improvement in properties achieved in LIBs through approaches like buffering of volume changes,

* Corresponding author at: School of Materials Science and Engineering, Nanyang Technological University, Singapore 639798, Singapore. Tel.: +65 6790 4140; fax: +65 6790 9081.
E-mail address: ashhhng@ntu.edu.sg (H.H. Hng).

0378-7753/$ – see front matter © 2012 Elsevier B.V. All rights reserved.
doi:10.1016/j.jpowsour.2011.12.064

supporting the anode material and prevention of aggregation of materials, or increasing electrical conductivity and prevention of direct contact of the anode material with the electrolyte. Works which focus on improving the performance of Ge-based anodes also include the formation of composites with carbon nanotubes or carbon coated Ge to buffer volume change [8,27], formation of Ge/Cu_3Ge/C composite to allow capacity retention by having amorphous carbon as a buffering matrix [3] and Cu_3Ge as the electrically conductive yet inactive phase [6], and sheathing of Ge nanowires with carbon [12]. The advantage of using Ge nanowires instead of other morphologies, apart from its ability to alloy with large amounts of lithium, is that it provides good electrical conductivity along the length of individual nanowires, short lithium ion diffusion distance and large interfacial area in contact with the electrolyte [12]. At the same time, the material is able to undergo facile strain relaxation, expanding freely in both radial and axial direction, such that good performance is able to be obtained [28].

Herein, we report a novel approach on the growth of Ge nanowires (Ge NW) in gold-seeded porous carbon via a solution–liquid–solid (SLS) mechanism, which to our best knowledge have not been reported yet. The electrochemical characteristics of the as-prepared samples are investigated using galvanostatic methods. The results showed improved performance in terms of reversible capacity, and improved cycling performance can be obtained in the porous carbon–Ge NW (PC–Ge NW) composite as compared to pure Ge NW. The presence of the porous carbon provides better electronic pathways and also acts as a buffering phase for the volume changes of Ge. Thus, at a current density of 160 mAg^{-1}, during the 50th cycle, pure Ge NW yields a specific capacity of 613 $mAhg^{-1}$, while the PC–Ge NW composite yields 789 $mAhg^{-1}$, which is a 28.7% improvement over the pure Ge NW anode. The advantages of using this solution phase synthesis method compared to other processes are that the Ge NW synthesized using this method can be collected in micrograms scale or scaled up as required for the preparation of the battery cell, the precursors and synthesis conditions required are also milder than in other reactions, and there is also less tendency for contamination which can occur through ball milling.

2. Materials and experimental procedures

2.1. Synthesis of germanium nanowires

In a typical Ge NW synthesis, 0.3 mL of diphenylgermane (DPG) and Au seeds (prepared according to Brust et al. [29]) in the molar ratio of Au:Ge being 1:350, were added to 40 mL of anhydrous cyclohexane in a glass beaker. Glass slides were added in as required to collect the NW, and the beaker was then placed in the high pressure high temperature (HPHT) reactor (Model: 4576, Parr Instrument Company), purged with argon gas for a few minutes and then sealed up. The reaction mixture was heated in the reactor to a temperature of about 633–643 K at a rate of about 3 $Kmin^{-1}$, left to react for a few minutes and then cooled to room temperature naturally. The as-synthesized Ge NW were collected by ultrasonication, centrifugation and vacuum-oven dried.

2.2. Synthesis of porous carbon–Ge nanowires composite

In the synthesis of PC–Ge NW, growth of gold seeds in porous carbon was first carried out: 10 mg porous carbon (Vulcon XC 72) was dispersed in 10 mL water and then mixed with 2 mL of 5 mM $HAuCl_4$. After 2 h, 1 mL of 0.1 M $NaBH_4$ was added and reacted for 1 h. The porous carbon–gold composite was separated by centrifugation and oven dried. The Ge NW were grown by mixing 10 mg porous carbon–gold with 0.1 mL DPG in 20 mL cyclohexane and reacted under the same conditions as the Ge NW growth.

2.3. Characterization

Phase identification of the pure Ge NW sample was carried out using X-ray diffraction (XRD) on Shimadzu X6000 using Cu K_α radiation (λ = 1.5418 Å), measured over diffraction angle 2θ from 20° to 75°, while the morphology was observed using a JEOL-JSM 7600F field emission scanning electron microscope (FESEM) and JEOL-JEM 2010 transmission electron microscope (TEM). Thermogravimetric analysis (TGA) (Model: Q500, TA Instruments) was carried out on the PC–Ge NW to determine the weight percent (wt.%) of Ge present.

2.4. Electrochemical measurements

Slurries for the PC–Ge NW and Ge NW were prepared as follows: (1) For PC–Ge NW: 80 wt.% PC–Ge NW composite material, 10 wt.% carbon black (as a conducting agent) and 10 wt.% polyvinylidene-fluoride (PVDF, which acts as a binder) were dissolved in N-methyl pyrrolidinone (NMP) (as a solvent). (2) For Ge NW: 70 wt.% of Ge NW, 20 wt.% carbon black and 10 wt.% PVDF were dissolved in NMP. The slurries were then coated on a copper foil and vacuum-oven dried at 333 K for 8 h. Electrochemical measurements were carried out on CR2032 coin-type cells with lithium foil as the counter electrode and reference electrode, Celgard 2400 membrane as the separator, and electrolyte solution obtained by dissolving 1 M $LiPF_6$ into a mixture of ethylene carbonate (EC) and dimethyl carbonate (DMC) (EC/DMC, 50:50 w/w). The coin cells were assembled in an Ar-filled glove box with concentrations of moisture and oxygen below 1.0 ppm. Cyclic voltammetry (CV) was performed with an electrochemical workstation (CHI 660C) at a scan rate of 0.5 mVs^{-1} and the charge–discharge tests were performed with a NEWARE battery tester at a current density of 160 mAg^{-1}, with a voltage window of 0.001–1.5 V.

3. Results and discussion

3.1. Phase identification and morphology

Fig. 1a shows the XRD patterns of the pure Ge NW and PC–Ge NW. It is shown that in both the XRD patterns, the peaks are indexed to cubic germanium (JCPDS no. 65-0333). There are no detectable GeO_2 peaks in the XRD patterns, which is advantageous since formation of GeO_2 on Ge NW is a problem faced in many solution phase syntheses [12]. Based on the TGA results obtained, the amount of Ge present is calculated to be 53.5 wt.%.

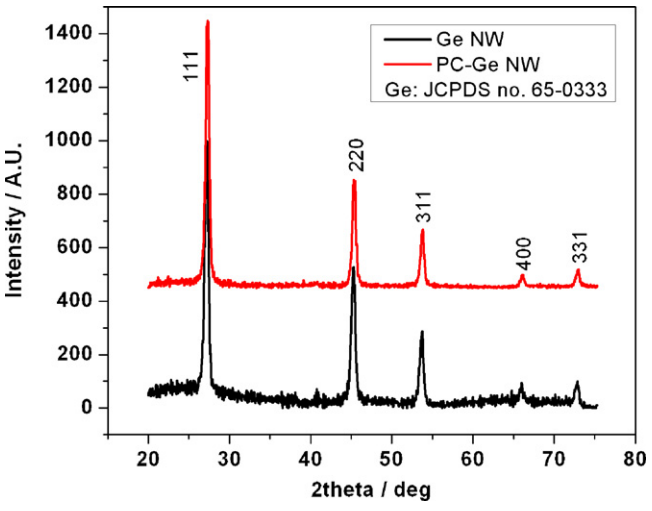

Fig. 1. XRD patterns of Ge NW and PC–Ge NW composite.

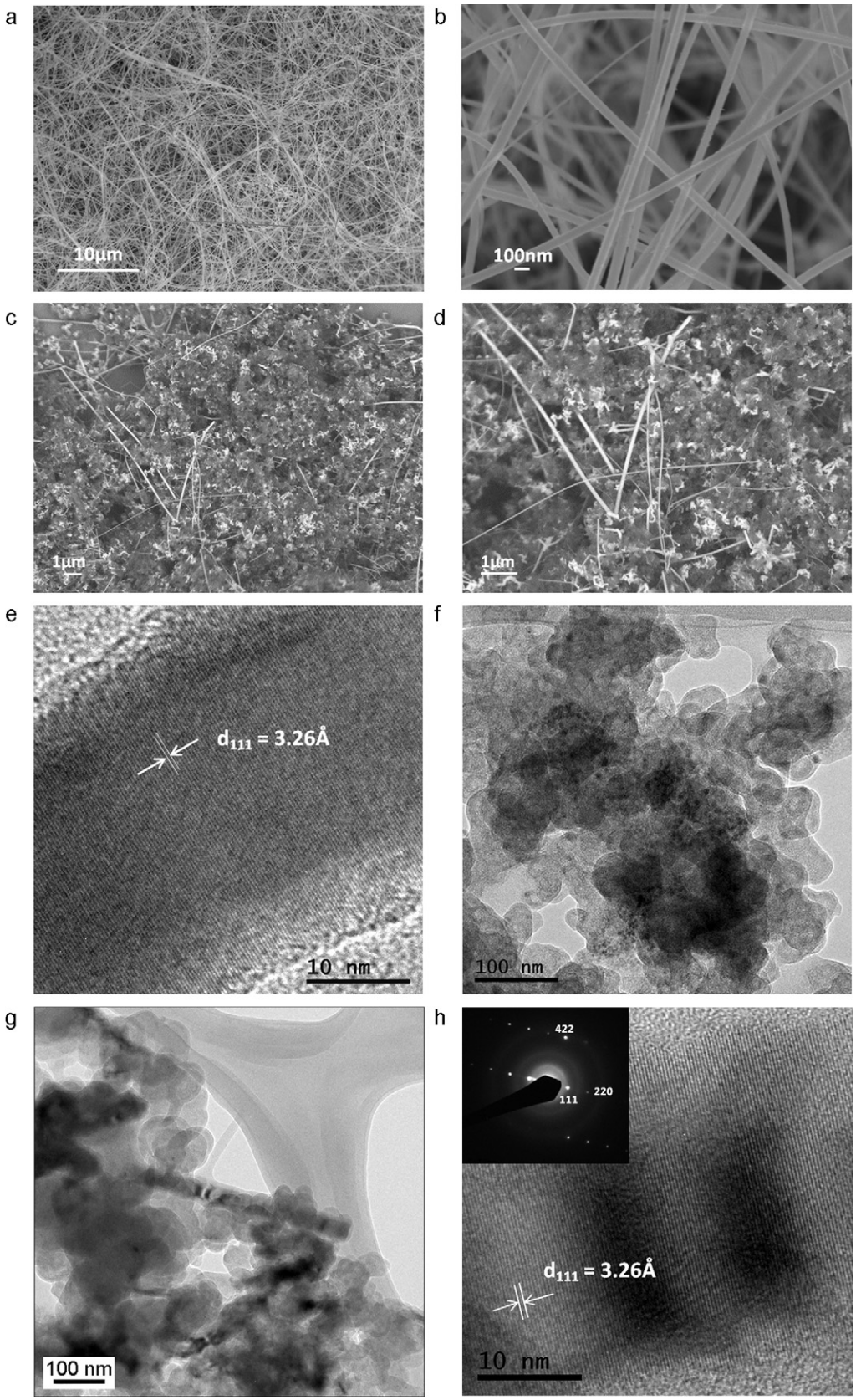

Fig. 2. FESEM images of Ge NW at (a) low magnification and (b) high magnification, and PC–Ge NW at (c) low magnification and (d) high magnification; TEM images of (e) Ge NW, (f) Ge NW dispersed in porous carbon, (g) close up of Ge NW embedded in porous carbon and (h) HRTEM showing the lattice fringes, and the inset shows the diffraction pattern.

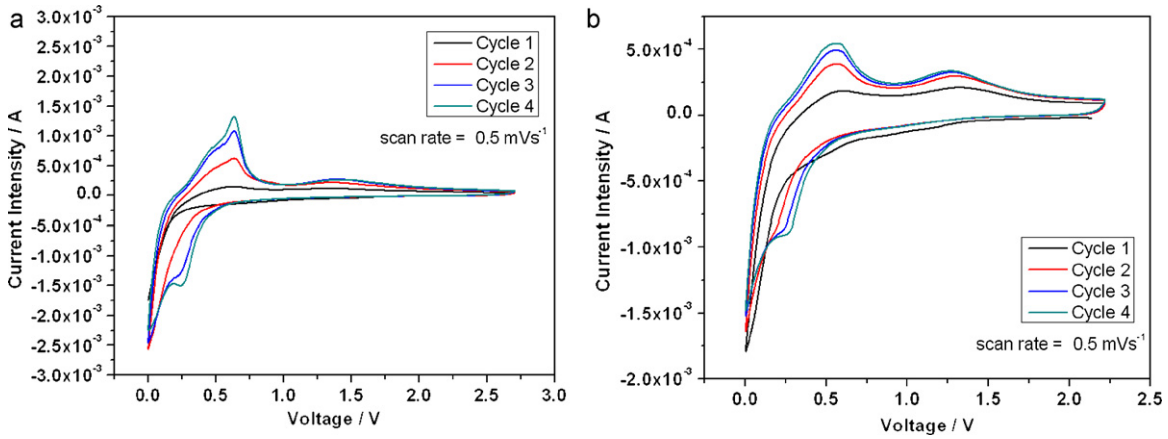

Fig. 3. CV profiles of (a) Ge NW and (b) PC–Ge NW composite.

The FESEM images of the Ge NW and PC–Ge NW are shown in Fig. 2a–d. The Ge NW are generally smooth with diameters in the range of 50 to 100 nm as observed in Fig. 2a and b, while Fig. 2c and d shows the Ge NW (bright regions) being dispersed in the porous carbon matrix (dark regions). Some portions of the Ge NW are extended out of the porous carbon, while some are embedded inside it. Fig. 2e–g shows the TEM images of the as-grown Ge NW, Ge NW (black spots or regions) dispersed in the porous carbon matrix and Ge NW being encapsulated by the porous carbon, respectively. The lattice fringes of the Ge NW in porous carbon are also observed in the high resolution TEM (HRTEM) image in Fig. 2h. Its d-spacing is 3.26 Å, corresponding to the (1 1 1) plane; the indexed diffraction pattern in the inset correlates to the various planes of Ge. Weak rings are also observed in the diffraction pattern, indicating the presence of the amorphous porous carbon.

3.2. Electrochemical measurements

The CV profiles of Ge NW and PC–Ge NW are shown in Fig. 3a and b. The redox peaks are observed at about 0.2 V, 0.6 V and between 1.2 and 1.4 V, indicating that Ge does react with Li in the 0–1.5 V region. The potential versus capacity profiles of the first cycle of the Ge NW and PC–Ge NW are shown in Fig. 4a. During the first cycle, the discharge and charge capacities are about 1787 $mAhg^{-1}$ and 915 $mAhg^{-1}$ respectively, for Ge NW, and 1393 $mAhg^{-1}$ and 865 $mAhg^{-1}$ respectively, for PC–Ge NW. Thus, for the PC–Ge NW sample, the discharge capacity, if based only on Ge, is 2604 $mAhg^{-1}$, which is much higher than the theoretical value of 1600 $mAhg^{-1}$ for Ge. Similar observation was also reported by Chan et al. [10], and it was attributed to the initial reactions at the surface of the Ge NW, e.g. formation of surface electrolyte interphase (SEI), leading to higher discharge capacity being observed. The first cycle Coulombic efficiency is about 51.2% for Ge NW, and 62.1% for PC–Ge NW, indicating that the addition of the carbonaceous phase increases the first cycle Coulombic efficiency. These values are within the range of the first Coulombic efficiency values reported for Ge ranging from about 30% to more than 90% [7–12]. Irreversible capacity is usually due to the formation of a SEI film from electrolyte decomposition, or due to the decomposition of the native oxide that forms on the Ge NWs, leading to an irreversible decomposition of GeO_2 to Ge and Li_2O [10]. For this work, as GeO_2 is not detected by XRD, the contribution to the irreversible capacity is assumed to be negligible. From the FESEM images, we see that in the composite sample, there is Ge NW being exposed, hence the formation of SEI would be the likely contribution to this irreversible capacity.

Fig. 4b compares the cycling performance of the two electrodes, where the PC–Ge NW composite gives a better cycling performance as compared to the Ge NW sample. For materials like Ge, massive volume change often leads to performance degradation. Although the first cycle capacity of both samples are high, reaching or nearly reaching the theoretical capacity, the capacity loss from the 2nd cycle of the samples differs, in the range of 33.2% to 42.4%, with Ge NW having the higher specific capacity of 1030 $mAhg^{-1}$ at the second cycle, and PC–Ge NW having the lower value at 930 $mAhg^{-1}$. This slight difference at the second cycle may be due to the presence of carbon, which has a low specific capacity. Nevertheless,

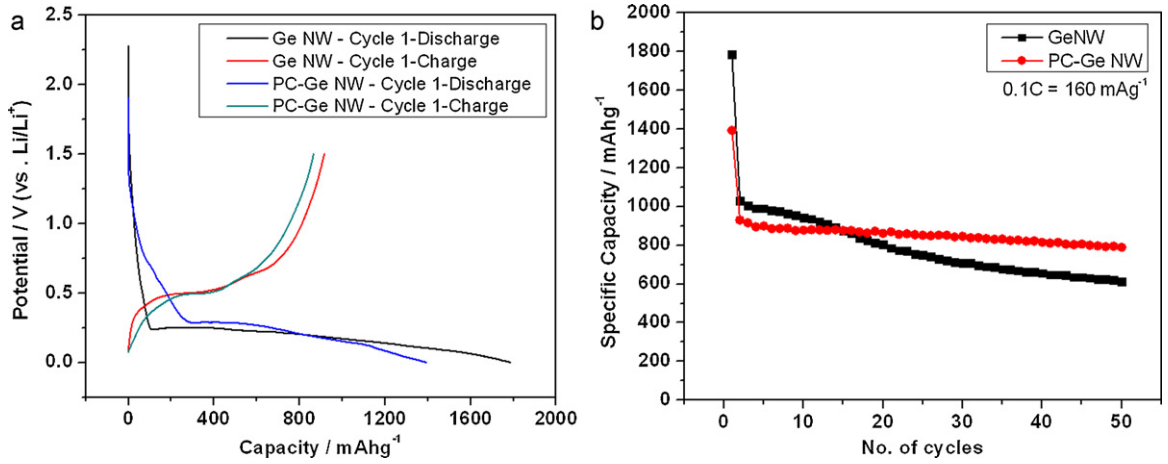

Fig. 4. (a) Potential versus capacity profile of the first cycle for Ge NW and PC–Ge NW composite; and (b) Specific capacity versus number of cycles.

as the number of cycles increase, the specific capacity of Ge NW decreases more quickly and continuously. PC–Ge NW, on the other hand, decreases very slightly after the 2nd cycle and it more or less maintains with a very gentle sloping line for the specific capacity, at values above that of the Ge NW sample.

From the trends observed, it is deduced that for the PC–Ge NW composite, expansion and contraction is less severe compared to Ge NW, due to the difference in structures. For PC–Ge NW composite, the NW is embedded within the porous carbon matrix, thus while it allows lithium ions to enter it to react with the Ge NW, it also buffers the volume change during the lithiation/delithiation process. On the other hand, for the pure Ge NW sample, the material is exposed fully, thus volume change during the lithiation and delithiation processes occurs freely; as such, the lack of the carbonaceous buffering phase for the volume changes in Ge NW contributes to its poor performance. The high initial discharge capacity of 1787 $mAhg^{-1}$ and 1393 $mAhg^{-1}$ are achieved for the Ge NW and PC–Ge NW composite respectively, and the reversible charge capacities are 1030 $mAhg^{-1}$ and 930 $mAhg^{-1}$, respectively. The specific capacity of the samples at the 50th cycle is 789 $mAhg^{-1}$ for PC–Ge NW and 613 $mAhg^{-1}$ for Ge NW, which is a 28.7% improvement. Based on calculations using the TGA results, the actual amount of Ge in PC–Ge NW is only 53.5 wt.%. Correlating this value to its performance at the 50th cycle, the capacity retention of the PC–Ge NW is 56.6% (based on the specific capacity at the first discharge cycle), while the capacity retention of Ge NW is 34.3%, indicating the synergistic effect provided by the presence of porous carbon. This discovery is beneficial as the presence of a lower amount of Ge can lead to good performance being maintained, and in turn this can lead to lower costs, which is a practical issue in the LIB industry.

It is reported that the presence of carbon as a coating is useful for improving the performance of electrode materials because it can serve as a buffer to cushion the stress induced on the anode material and mitigate the aggregation of the material during cycling. Carbon coating can also increase the electronic conductivity of the electrodes [22], and these are supported by the results in this work. The presence of porous carbon, and the fact that the Ge NW is embedded inside it, allows the Ge NW to be shielded from the electrolyte. As such, the amount of SEI that forms is reduced, and correspondingly, the efficiency increases and irreversible capacity decreases.

Good results have also been reported by Chan et al. [10] and Seo et al. [12] on the performance of Ge NW for LIB applications. Compared to their works, the performance obtained here is comparable. In addition, for this work, the Ge NW are grown directly inside the gold-seeded porous carbon using a simple and widely studied solution phase synthesis method, without the need for an additional step of carbon coating on Ge NW through a specialized experimental set up and precursor. The method used in this work also avoids the use of the VLS mechanism, which has limitations when it comes to scaling up. In addition, this method is a milder and simpler approach as compared to the other synthesis methods of Ge–carbon composites like mechanical milling and pyrolysis [3,6,8,27].

To verify the improved anode performance properties of the PC–Ge NW composite, rate capabilities are measured on the sample at 160 mAg^{-1}, 320 mAg^{-1}, 800 mAg^{-1}, 1600 mAg^{-1}, and back to 800 mAg^{-1} and 160 mAg^{-1}, respectively. As seen in Fig. 5, the cycling performance of the sample is relatively stable at each discharge rate, and is able to maintain a specific capacity of 450 $mAhg^{-1}$ at 1600 mAg^{-1}. Upon return to cycling rates of 800 mAg^{-1} and 160 mAg^{-1}, the specific capacity decreases only slightly, and so this material can be operated at higher discharge rates. The inset shows the electrochemical impedance spectroscopy (EIS) of the two samples, with a lower impedance value observed for the PC–Ge NW sample. This is due to improved electronic transport contributed by the addition of porous carbon, resulting in better performance in the composite sample compared to pure Ge NW, and also reduces the capacity loss at high discharge rates.

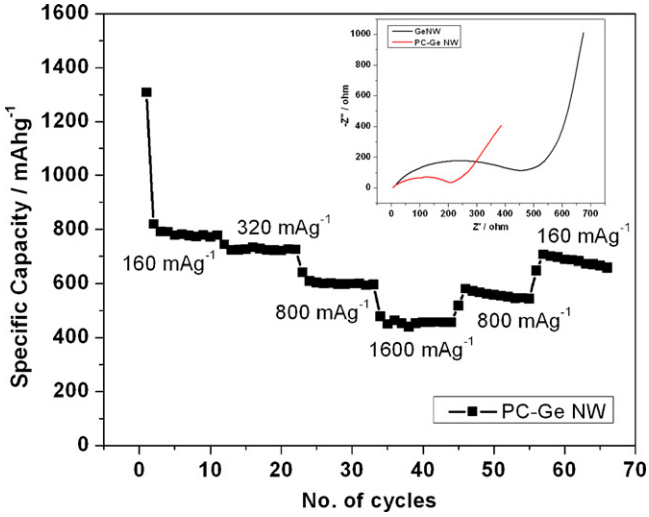

Fig. 5. Cycling performance of PC–Ge NW at varying discharge rates, with the EIS in the inset.

4. Conclusion

In conclusion, a novel approach on the growth of Ge NW in porous carbon via a SLS mechanism was reported for forming a PC–Ge NW composite. Comparing the performance achieved using Ge NW as anode and the PC–Ge NW composite as anode, an improvement of 28.7% in the specific capacity is achieved for PC–Ge NW over the Ge NW at the 50th cycle. In addition, the presence of only 53.5 wt.% of Ge in the sample allows a high specific capacity to be reached. At the 50th cycle, PC–Ge NW composite is able to maintain 56.6% of the initial reversible capacity, compared to only 34.3% for pure Ge NW. The results presented here is important as the presence of a lower amount of Ge can allow good performance to be maintained, and this in turn can lead to lower costs, which is a practical issue in the LIB industry. Nevertheless, further work has to be done to get the optimized ratio of porous carbon: Ge for improved cycling performance and capacity retention. This synthesis protocol can also be used for synthesis of other nanowires, like silicon, which has similar reaction mechanism as Ge, and good cycling properties are also expected.

Acknowledgements

The authors gratefully acknowledge AcRF Tier 1 RG 31/08 of MOE (Singapore), NRF2009EWT-CERP001-026 (Singapore), Singapore Ministry of Education (MOE2010-T2-1-017), A*STAR SERC grant 1021700144 and Singapore MPA 23/04.15.03 RDP 009/10/102 and MPA 23/04.15.03 RDP 020/10/113 grant.

References

[1] L.W. Ji, Z. Lin, M. Alcoutlabi, X.W. Zhang, Energy & Environmental Science 4 (2011) 2682–2699.
[2] J. Baxter, Z. Bian, G. Chen, D. Danielson, M.S. Dresselhaus, A.G. Fedorov, T.S. Fisher, C.W. Jones, E. Maginn, U. Kortshagen, A. Manthiram, A. Nozik, D.R. Rolison, T. Sands, L. Shi, D. Sholl, Y. Wu, Energy & Environmental Science 2 (2009) 559–588.
[3] Y. Hwa, C.M. Park, S. Yoon, H.J. Sohn, Electrochimica Acta 55 (2010) 3324–3329.
[4] L. Baggetto, P.H.L. Notten, Journal of the Electrochemical Society 156 (2009) A169–A175.
[5] C.M. Park, J.H. Kim, H. Kim, H.J. Sohn, Chemical Society Reviews 39 (2010) 3115–3141.
[6] O.B. Chae, S. Park, J.H. Ku, J.H. Ryu, S.M. Oh, Electrochimica Acta 55 (2010) 2894–2900.

[7] L.C. Yang, Q.S. Gao, L. Li, Y. Tang, Y.P. Wu, Electrochemistry Communications 12 (2010) 418–421.
[8] G.L. Cui, L. Gu, N. Kaskhedikar, P.A. van Aken, J. Maier, Electrochimica Acta 55 (2010) 985–988.
[9] Y.D. Ko, J.G. Kang, G.H. Lee, J.G. Park, K.S. Park, Y.H. Jin, D.W. Kim, Nanoscale 3 (2011) 3371–3375.
[10] C.K. Chan, X.F. Zhang, Y. Cui, Nano Letters 8 (2008) 307–309.
[11] H. Lee, H. Kim, S.G. Doo, J. Cho, Journal of the Electrochemical Society 154 (2007) A343–A346.
[12] M.H. Seo, M. Park, K.T. Lee, K. Kim, J. Kim, J. Cho, Energy & Environmental Science 4 (2011) 425–428.
[13] H. Lee, M.G. Kim, C.H. Choi, Y.K. Sun, C.S. Yoon, J. Cho, Journal of Physical Chemistry B 109 (2005) 20719–20723.
[14] I. Sandu, P. Moreau, D. Guyomard, T. Brousse, L. Roue, Solid State Ionics 178 (2007) 1297–1303.
[15] G.L. Cui, L. Gu, L.J. Zhi, N. Kaskhedikar, P.A. van Aken, K. Mullen, J. Maier, Advanced Materials 20 (2008) 3079–3083.
[16] J. Saint, M. Morcrette, D. Larcher, L. Laffont, S. Beattie, J.P. Peres, D. Talaga, M. Couzi, J.M. Tarascon, Advanced Functional Materials 17 (2007) 1765–1774.
[17] H. Kim, B. Han, J. Choo, J. Cho, Angewandte Chemie-International Edition 47 (2008) 10151–10154.
[18] W. Xu, N.L. Canfield, D.Y. Wang, J. Xiao, Z.M. Nie, J.G. Zhang, Journal of Power Sources 195 (2010) 7403–7408.
[19] S. Bourderau, T. Brousse, D.M. Schleich, Journal of Power Sources 81 (1999) 233–236.
[20] S. Yoon, S.I. Lee, H. Kim, H.J. Sohn, Journal of Power Sources 161 (2006) 1319–1323.
[21] Y.S. Hu, R. Demir-Cakan, M.M. Titirici, J.O. Muller, R. Schlogl, M. Antonietti, J. Maier, Angewandte Chemie-International Edition 47 (2008) 1645–1649.
[22] Y.M. Liu, X.Y. Zhao, F. Li, D.G. Xia, Electrochimica Acta 56 (2011) 6448–6452.
[23] J. Wang, H.L. Zhao, J.C. He, C.M. Wang, Journal of Power Sources 196 (2011) 4811–4815.
[24] J. Wang, H.L. Zhao, X.T. Liu, C.M. Wang, Electrochimica Acta 56 (2011) 6441–6447.
[25] M. Yang, Q.M. Gao, Microporous and Mesoporous Materials 143 (2011) 230–235.
[26] P. Zhang, Z.P. Guo, Y.D. Huang, D.Z. Jia, H.K. Liu, Journal of Power Sources 196 (2011) 6987–6991.
[27] S. Yoon, C.M. Park, H.J. Sohn, Electrochemical and Solid-State Letters 11 (2008) A42–A45.
[28] G.K. Simon, T. Goswami, Metallurgical and Materials Transactions a-Physical Metallurgy and Materials Science 42A (2011) 231–238.
[29] M. Brust, M. Walker, D. Bethell, D.J. Schiffrin, R. Whyman, Journal of the Chemical Society-Chemical Communications (1994) 801–802.